A Novel Class of High-T_C Ferromagnetic Semiconductors

Novel Ferromagnetic Semiconductors

L. V. Shlyk, S. A. Kryukov and L. E. De Long
Department of Physics and Astronomy
University of Kentucky
Lexington, KY 40506-0055 U.S.A.

J. W. Lynn and Qing Huang
NIST Center for Neutron Research
Gaithersburg, MD U.S.A.

B. Schüpp-Niewa and R. Niewa
Department Chemie
Technischen Universität
München, Germany

E. Arenholz and C. Piamonteze
Advanced Light Source
Lawrence Berkeley National Laboratory
Berkeley, CA U.S.A.

Abstract— We have grown single crystals of novel ruthenates $(Sr,Ba)(Fe,Co)_{2+x}Ru_{4-x}O_{11}$ that exhibit long-range ferromagnetic order well above room temperature, accompanied by narrow-gap semiconducting properties that include a large anomalous Hall conductance, low resistivity, high carrier concentration and low coercive field, which are properties well suited to spintronic applications. X-ray diffraction, EDX, neutron diffraction and x-ray absorption measurements on single crystals firmly establish the "R-Type" hexagonal ferrite structure (space group $P6_3/mmc$, No 194) and single-phase nature of all samples. The electronic structure and physical properties can be tuned by simple chemical substitution of two elements, M = Fe or Co, or by varying the relative concentration of 3d solutes and 4d Ru. Our magnetotransport, x-ray magnetic circular dichroism and magnetic moment data suggest the mechanism for FM order is quite different from that governing known dilute magnetic semiconductors.

Keywords- Spintronics, ferromagnetic semiconductors, ruthenates, mechanisms of ferromagnetism, R-Type ferrites

I. INTRODUCTION

The anticipation of revolutionary advances in nanoelectronics and information technologies has stimulated an intensive effort to discover new materials for spin-transport electronics ("spintronics"), in which the spin of charge carriers provides enhanced functionality for sub-micron devices [1,2]. The injection of spin-polarized electrons from a ferromagnetic (FM) metal into a semiconductor in a metal/semiconductor heterostructure poses difficult problems related to differences in conductivity and spin relaxation time in metals and semiconductors [3]. The injection of spin-polarized currents into semiconductor electronics therefore requires a highly transmissive (i.e., no impedence mismatch) interface between a non-magnetic semiconductor and a room-temperature, FM semiconductor (FS). If suitable materials can be discovered, room-temperature FS will underpin a variety of novel devices, including spin-based field effect transistors, spin-based light emitting diodes, and nanoscale MRAM [4,5].

"Dilute magnetic semiconductors" (DMS), such as (Ga,Mn)As and (Zn,Co)O, are intensively studied prospects for spintronics [4,5]. However, the weak solubility of 3d magnetic ions in these semiconductor hosts promotes clustering of the magnetic dopants, an inhomogeneous FM state, and large gradients of electrical conductivity [6,7] that have so far made DMS unsuitable for devices; moreover, experimental data and theoretical descriptions for DMS remain controversial [8,9]. The "half-metallic" 3d-oxides CrO_2 and Fe_3O_4 support high Curie-temperatures [10]; however, these materials possess thermodynamically driven defects that have so far inhibited device fabrication [11-13]. Therefore, it is crucial to discover high-T_c FS based on a periodic array of magnetic ions.

We have grown single crystals of a novel family of ruthenates $(Sr,Ba)(Fe,Co)_{2+x}Ru_{4-x}O_{11}$ that exhibit long-range FM order well above room temperature, accompanied by narrow-gap semiconducting properties that include a large anomalous Hall conductance, low resistivity, high carrier concentration and low coercive field, which are properties well suited to spintronic applications [14-16]. A short overview of the physical and chemical properties of this new class of FS is given below.

II. EXPERIMENTAL RESULTS

A. Sample Preparation and Structure

Polycrystalline samples of $BaFe_2Ru_4O_{11}$ were previously synthesized [17], but only sparse data for the physical properties of $BaFe_2Ru_4O_{11}$ and $BaMn_2Ru_4O_{11}$ were reported [17]. These compounds form within the "R-Type" hexagonal ferrite structure (space group $P6_3/mmc$, No 194; see Fig. 1) [18], which consists of layers of edge-sharing $M(2)O_6$ octahedra interspaced by layers of face-sharing $M(1)O_6$ octahedra and $M(3)O_3$ trigonal bipyramids (see Fig. 1). Note that the magnetic Fe, Co and Ru ions of $(Sr,Ba)(Fe,Co)_2Ru_4O_{11}$ reside on a periodic sublattice, in contrast to dilute magnetic semiconductors (DMS) [14-16].

We have grown single crystals of novel ruthenates $(Sr,Ba)(Fe,Co)_{2+x}Ru_{4-x}O_{11}$, as described elsewhere [14,15]. We find that single crystals form at compositions that differ from previously investigated polycrystalline materials [17,18]. For example, x-ray refinements on two single-crystals yielded compositions $BaFe_{3.39(5)}Ru_{2.61(5)}O_{11}$ and $BaCo_{1.85(6)}Ru_{4.15(6)}O_{11}$ and different occupations for the two sites M(1) (e.g., $Fe_{0.64(1)}/Ru_{0.36}$ or $Co_{0.10(1)}/Ru_{0.90}$) and M(2) (e.g., $Fe_{0.37(1)}/Ru_{0.63}$ or $Co_{0.22(1)}/Ru_{0.78}$), which also lead to important variations in physical properties [14-16]. Nevertheless, microprobe analyses yield a stable stoichiometric ratio n(M)/n(Ba) = 6.0 for BaM_6O_{11} for every investigated sample.

B. Magnetic Properties

Single-crystal $BaCo_{1.85(6)}Ru_{4.15(6)}O_{11}$, exhibits soft ferromagnetism below T_c = 105 K, but with a strongly anisotropic susceptibility that obeys a modified Curie-Weiss law above 150 K, with a temperature-independent term χ_0 = 3.8 x 10^{-3} emu/mol, θ_p = 115 K (70 K), and μ_{eff} = 3.08 μ_B (2.41 μ_B) for H || c (H ⊥ c). Curie-Weiss fits using a spatial average $\chi = (\chi_{||} + 2\chi_{\perp})/3$ yield μ_{eff} = 2.78 μ_B. Using $\mu_{eff} = [n_1\mu_1(Co^{2+})^2 + n_2\mu_2(Ru^{3+})^2 + n_3\mu_3(Ru^{5+})^2]^{1/2}$, where n_1, n_2 and n_3 are the respective mole fractions of Co^{2+}, Ru^{3+} and Ru^{5+} from x-ray refinements, and μ_i the respective atomic moments for spin-only Co^{2+} (S = 1/2), Ru^{3+}(S = 1/2) and Ru^{5+} (S = 3/2), yields an effective moment μ_{eff} = 2.81 μ_B that corroborates the mixed valence of Ru [14].

In contrast, $BaFe_{3.39(5)}Ru_{2.61(5)}O_{11}$ develops FM order at a remarkable T_c = 440 K that was too high to extract Curie-Weiss parameters (due to the limitations of our Quantum Design MPMS5 SQUID Magnetometer). $BaFe_{3.4}Ru_{2.6}O_{11}$ is a soft ferromagnet with saturation moment μ_S = 1.25 μ_B/f.u., and coercive fields $H_{C||}$ = 480 Oe and $H_{C\perp}$ = 92 Oe at T = 300 K [14,15]. Note that the magnetization anisotropy $(m_\perp/m_{||} \approx 1.5$ at T = 5 K) of $BaFe_{3.4}Ru_{2.6}O_{11}$ is reduced by more than two orders of magnitude, and the easy axis shifts from the ab-plane to the c-direction, compared to $BaCo_{1.85}Ru_{4.15}O_{11}$ (see Table 1, below).

We also discovered the novel Sr-based ferrites $SrFe_{2+x}Ru_{4-x}O_{11}$ (Figs. 2 and 3) are FM (or possibly ferrimagnetic) at temperatures as high as 488 K [15,16]. Replacement of Co for Fe lowers T_C, as shown by FC χ(T) data for $BaCo_{1.8}Ru_{4.2}O_{11}$ (T_C = 105 K) and $SrCo_2Ru_4O_{11}$ (T_C = 115 K) single crystals (see Table 1). These compounds are very soft ferromagnets ($H_c \approx 1$ Oe at T = 80 K) with saturation moments $\mu_S \approx 1.8 \pm 0.1$ μ_B/f.u. at T = 5 K and easy axes within the ab-plane. Above 150 K, both $BaCo_{1.8}Ru_{4.2}O_{11}$ and $SrCo_2Ru_4O_{11}$ follow modified Curie-Weiss laws with positive Weiss constants. Spatial averages $\chi = (\chi_{||} + 2\chi_{\perp})/3$ of the Curie-Weiss susceptibilities above 150 K yield effective magnetic moments, μ_{eff} = 2.78 μ_B ($BaCo_{1.8}Ru_{4.2}O_{11}$) and μ_{eff} = 2.84 μ_B ($SrCo_2Ru_4O_{11}$), near the values 2.81 μ_B and 2.74 μ_B, resp., obtained using compositions from X-ray refinements and theoretical spin-only values for Ru^{3+}(S = 1/2), Ru^{5+}(S = 3/2) and Co^{2+} (S = 1/2). We again could not extract accurate Curie-Weiss parameters for the $SrFe_{2+x}Ru_{4-x}O_{11}$ analogues due to their very high T_C's.

Atomic substitutions may produce inhomogeneities in magnetization and electrical conductivity (as in DMS), which is detrimental to spintronic applications since a sufficiently large and uniform carrier spin polarization is needed for effective spin injection. For example, the anomalous Hall effect and magnetization of $SrFe_{2.6}Ru_{3.4}O_{11}$ do not saturate at an applied field of 5 T (see Fig. 2), which may indicate canted or other complex FM order, or short-range magnetic order above T_C, as observed in DMS such as (Ga,Mn)As [19].

The magnetization distribution and the temperature dependence of the FM order parameter can be assessed via elastic magnetic neutron scattering. We have just obtained magnetic diffraction data for a small crystal of $SrFe_{2.6}Ru_{3.4}O_{11}$, to deduce the temperature dependence of the ordered moment (see Fig. 3). Additional magnetic powder diffraction experiments are underway to assess the magnetic homogeneity and structure of selected sample compositions from complete linewidth and intensity analyses.

C. Magnetotransport Properties

Variations of the 3d (Co,Fe) and 4d (Ru) contents have profound effects on the magnetotransport properties of the R-Type ferrites [14-16], as summarized in Table 2. The in-plane and out-of plane resistivities ($\rho_{||300}$ = 3.9 x 10^{-4} Ω·cm and $\rho_{\perp 300}$ = 1.4 x 10^{-4} Ω·cm, respectively) of single-crystal $BaCo_{1.8}Ru_{4.2}O_{11}$ are clearly metallic ($d\rho/dT > 0$) (Fig. 4). The Curie temperature is marked by a drop-off of ρ(T) at ~ 105 K, above which the in-plane resistivity has strong linear temperature dependence similar to that of high-temperature cuprate superconductors, and considered a signature of strongly correlated or marginal Fermi liquid physics. In contrast, ρ(T) of single-crystal $SrCo_2Ru_4O_{11}$ increases with decreasing T, consistent with a small semiconducting gap ($\Delta \sim 1.1$ meV) that is abruptly reduced below T_C (Fig. 4). The slopes $d\rho/dT < 0$ indicate semiconductivity of all single-crystal Fe-based Ba- and Sr-ferrites with an activated form $\rho(T) = \rho_0 e^{\Delta/kT}$ and narrow gaps $\Delta \approx$ 10-60 meV for current both parallel ($\rho_{||}$) or perpendicular ($\rho_\perp$) to the ab-plane (Table 2). The room-temperature resistivities ρ_{300} of the Ba- and Sr-based Fe ferrites are in the range of typical narrow-gap semiconductors (0.001-100 Ω·cm), and therefore have the potential to optimize the spin injection and detection efficiencies across a doped-semiconductor/FS interface.

The Hall resistivity $\rho_H = R_0H + 4\pi MR_s$ in ferromagnets, where R_0 is the Hall coefficient resulting from the Lorentz force on the carriers, and R_s is the anomalous Hall coefficient that depends on the magnetization and spin-orbit coupling [20-22]. Therefore, ρ_H has roughly the same field dependence as the magnetization in ferromagnets below T_c [20], as demonstrated by single-crystal $BaFe_{3.4}Ru_{2.6}O_{11}$ and $SrFe_{2.6}Ru_{3.4}O_{11}$ for H << 1.0 T and T ≤ T_c (Fig. 6). The anomalous contribution to ρ_H(H) of $BaFe_{3.4}Ru_{2.6}O_{11}$ is ≈ 70 μΩ cm, which is much larger than those of metallic or semiconducting ferromagnets such as (Ga,Mn)As [23] and $Fe_{1-x}Co_xSi$ [24], and indicates a strong, net carrier spin polarization

that is requisite for an ideal FS injecting contact. The magnetization of $BaFe_{3.4}Ru_{2.6}O_{11}$ saturates above 1.0 T, and consequently ρ_H becomes much less field dependent with $d\rho_H/dH = R_0 = 1/nec$, where n is the carrier concentration. The positive slope of the $\rho_H(H)$ curve at T = 300 K and $\mu_o H > 1.0$ T reveals the dominant charge carriers in single-crystal $BaFe_{3.4}Ru_{2.6}O_{11}$ are holes (Fig. 6) with density $n \approx 2 \times 10^{21}$ cm^{-3} and mobility $\mu_H = R_0/\rho \approx 4$ $cm^2V^{-1}s^{-1}$. The $\rho_H(H)$ observed for single-crystal $BaCo_{1.8}Ru_{4.2}O_{11}$ and $SrCo_2Ru_4O_{11}$ have negative slopes that indicate the dominant charge carriers are electrons, which is distinctly different from the p-type Fe-based ferrites. A carrier concentration $n \approx 3 \times 10^{20}$ cm^{-3} and mobility $\mu_H \approx 55$ $cm^2/V^{-1}s^{-1}$ can be estimated from the ordinary Hall coefficient at T = 120 K for $BaCo_{1.8}Ru_{4.2}O_{11,}$ and $n \approx 1 \times 10^{21}$ cm^{-3} and $\mu_H \approx 2.8$ cm^2 $V^{-1}s^{-1}$ at T = 150 K for $SrCo_2Ru_4O_{11}$ (see Table 2).

Subtle crystal/chemical variations could underly the surprisingly varied behavior of the R-Type ferrites [14]. An intermediate or mixed valence state for a magnetic element can lead to unusual physical properties [25,26], and are frequently observed for ruthenates [27]. Our x-ray refinements, SQUID magnetometer data, and charge balance considerations imply Co2+, mixed Ru3+/Ru5+ and Fe2+/Fe3+ are present in single-crystal BaFe3.4Ru2.6O11 and BaCo1.9Ru4.1O11 [14]. Additional x-ray absorption (XA) spectra and x-ray magnetic circular dichroism (XMCD) experiments were performed at beamline 6.3.1 of the Advanced Light Source. XA spectra were recorded in total electron yield mode probing the topmost 5–10 nm of the sample and XMCD spectra were obtained in applied fields of 0.2 T. XA data for single-crystal SrFe2.6Ru3.4O11 and BaCo2Ru4O11 are shown in Figs. 7 and 8(a) are consistent with mixed valent (+2,+3) Fe and Co oxidation states. Such differences between XAS, magnetometer and x-ray diffraction data may reflect strongly composition- or temperature-dependent oxidation states and/or significant sensitivity of the surface near region probed by soft x ray absorption spectroscopy to exposure to air that must be checked in future experiments.

III. Discussion

An especially attractive characteristic of R-Type Ru ferrites is that their magnetic and electrical properties can be widely varied by substitution of Fe for Ru over a homogeneity range $(Ba,Sr)Fe_{2\pm x}Ru_{4 \mp x}O_{11}$, or Co for Fe within the solid solutions $(Ba,Sr)(Co,Fe)_{2\pm x}Ru_{4 \mp x}O_{11}$. The concomitant increases of the semiconducting gap and Curie temperature, and decrease of magnetic anisotropy, with increasing Fe content suggest a close relationship exists between the magnetic interactions and the resistivity behavior (see Tables 1 and 2). The Co- or Fe-concentration dependences of T_C and Δ of polycrystalline $Sr(Fe_{1-y}Co_y)_{2\pm x}Ru_{4\pm x}O_{11}$ and single-crystal $SrFe_{2\pm x}Ru_{4\pm x}O_{11}$, are shown in Fig. 9. Increasing the Co^{2+} ($3d^7$) concentration produces an evolution from a high-T_C, p-type FS to a low-T_C FM metal, which demonstrates that the wider the semiconducting gap the higher the Curie temperature. This intriguing trend is opposite to that observed for DMS (where an increase in carrier concentration leads to higher T_C, but also to higher metallicity), and is an important clue concerning the mechanism of high-T_C ferromagnetism in the R-Type ferrites [15].

IV. Conclusion

The discovery of new materials often leads to new or improved technologies with substantial commercial value---especially if properties of interest can be widely varied and precisely controlled. We have demonstrated that the R-Type ferrite FS can accommodate broad variations of electric and magnetic properties via simple substitution of the 3d-4d metal concentrations. The stability range and physical properties of $(Ba,Sr)M_{2\pm x}Ru_{4 \mp x}O_{11}$ materials are not completely known, and the physical properties of samples covering a wider range of compositions with $M = (Fe_{1-x}Co_x)$ are under investigation.

The Advanced Light Source is supported by the Director, Office of Science, Office of Basic Energy Sciences, of the U.S. Department of Energy under Contract No. DE-AC02-05CH11231.

References

[1] D. Grundler, “Spintronics”, *Physics World*, April, 2002, page 39.

[2] D. Awschalom, M. Flatté and N. Samarth, “Spintronics”, *Scientific American*, June, 2002, page 67.

[3] X. Jiang, R. Wang, R. M. Shelby and S. S. P. Parkin, “Highly efficient room temperature tunnel spin injector using CoFe/MgO(001)”, IBM J. Res., vol. 50, pp. 111-120, 2006.

[4] I. Zutic, J. Fabian and S. Das Sarma, Rev. Mod. Phys., vol. 76, pp. 323-410, 2004.

[5] D. D. Awschalom and M. E. Flatté., Nature Physics, vol. 3, pp. 153-159. 2007.

[6] T. Dietl, “Origin and control of high temperature ferromagnetism in semiconductors”, J. Appl. Phys., in press, 2008.

[7] M. J. Coey, “Dilute Magnetic Oxides”, J. Appl. Phys., in press, 2008.

[8] J. C. A. Huang, H. S. Hsu, Y. M. Hu, C. H. Lee, Y. H. Huang and M. Z. Lin, “Origin of ferromagnetism in ZnO/CoFe multilayers: Diluted magnetic semiconductor or clustering effect?”, Appl. Phys. Lett., vol. 85, pp. 3815-3817, 2004.

[9] T. Hynninen, H. Raebiger, J. von Boehm and A. Ayuela, “High Curie temperatures in (Ga,Mn)N from Mn clustering”, Appl. Phys. Lett., Vol. 88, pp. 122501-122503, 2006.

[10] W. E. Pickett and J. S. Moodera, “Half-metallic magnets”, *Physics Today*, vol. 54, pp. 39-44, 2001.

[11] Xiaojing Zou and Gang Xiao, “Magnetic domain configurations of epitaxial chromium dioxide (CrO_2) nanostructures”, Appl. Phys. Lett., vol. 91, page 113512, 2007.

[12] K. Balakrishnan, S. K. Arora and I. V. Shvets, “Strain relaxation studies of the Fe_3O_4/MgO(100) heteroepitaxial system grown by magnetron sputtering”, J. Phys. Conden. Mat., vol. 16, page 5387, 2004.

[13] W. L. Zhou, K.-Y. Wang, C. J. O’Connor and J. Tang, “Granular growth of Fe_3O_4 thin films and its antiphase boundaries prepared by pulsed laser deposition”, J. Appl. Phys., vol. 89, page 7398, 2001.

[14] B. Schüpp-Niewa, L. Shlyk, S. Kryukov, L. De Long and R. Niewa, “$BaFe_{3.39(5)}Ru_{2.61(5)}O_{11}$ and $BaCo_{1.85(6)}Ru_{4.15(6)}O_{11}$: preparation, single crystal structure refinements, magnetic and transport properties of quaternary transition metal oxoruthenates”, Zeit. Naturforsch. B, vol. 62, pp. 753-758, 2007.

[15] L. Shlyk, S. Kryukov, B. Schupp-Niewa, R. Niewa and L. E. De Long, “High temperature ferromagnetism and tunable semiconductivity of

(Ba,Sr)$M_{2\pm x}Ru_{4\pm x}O_{11}$: a new paradigm for spintronics", Adv. Mat., vol. 20, pp. 1315-1320, 2008.

[16] L. Shlyk, L. E. De Long, S. Kryukov, B. Schupp-Niewa and R. Niewa, "High temperature ferromagnetism and tunable semiconductivity of $SrM_{2\pm x}Ru_{4\pm x}O_{11}$", J. Appl. Phys., vol. 103, page 07D112, 2008.

[17] M. C. Cadee and D. J. W. Ijdo, "Refinement of the 6-layer structures of the R-type hexagonal ferrites $BaTi_2Fe_4O_{11}$ and $BaSn_2Fe_4O_{11}$", J. Solid State Chem., vol. 52, pp. 302-312, 1984.

[18] M. L. Foo, Q. Huang, J. W. Lynn, Wei-Li Lee, T. Klimczuk, I. S. Hagemann, N. P. Ong, R. J. Cava, J. Solid State Chem., vol. 179, page 563, 2006.

[19] H. Ohno, "Making nonmagnetic semiconductors ferromagnetic", *Science*, vol. 281, pp. 951-956, 1998.

[20] N. Manyala, et al., "Magnetoresistance from quantum interference effects in ferromagnets", *Nature*, vol. 404, pp. 581-584, 2000.

[21] R. Karplus and J. M. Luttinger, "Hall effect in ferromagnetics", Phys. Rev. B, vol. 95, pp. 1154-1160, 1954.

[22] L. Berger, "Side-jump mechanism for the Hall effects of the ferromagnets", Phys. Rev. B, vol. 2, pp. 4559-4556, 1970.

[23] F. Matsukara, H. Ohno, A. Shen, and Y. Sugawara, "Transport properties and origin of ferromagnetism in (Ga,Mn)As", Phys. Rev. B, vol. 57, pp. R2037-R2040, 1998.

[24] N. Manuala, Y. Sidis, F. G. DiTusa, G. Aeppli, D. P. Young and Z. Fisk, "Large anomalous Hall effect in a silicon-based magnetic semiconductor", Nature Materials, vol. 3, pp. 255-262, 2004.

[25] D. K. Wohlleben and B. R. Coles, "Formation of Local Magnetic Moments in Metals: Experimental Results and Phenomenology" in: Magnetism, vol. V, H. Suhl, Ed. New York: Academic Press, 1973, Chapt. 1.

[26] M. B. Maple, L. E. DeLong and B. C. Sales, "Kondo Effect: Alloys and Compounds" in: Handbook on the Physics and Chemistry of Rare Earths, vol. 1, Karl A. Gschneidner, Jr., and LeRoy Eyring, Eds. Amsterdam: North Holland, 1978), Chapt. 11.

[27] Hk. Müller-Buschbaum, Z. Anorg. Allg. Chem., vol. 632, page 1625, 2006.

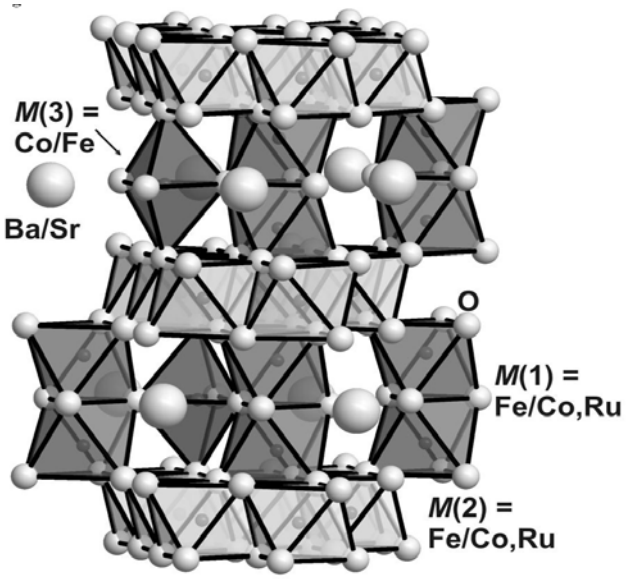

Fig. 1. $(Ba,Sr)M_{2\pm x}Ru_{4\pm x}O_{11}$ (M = Fe, Co) crystal structure: Layers of $M(2)O_6$ (octahedra are connected in the [001] direction via $M(1)_2O_9$ double-octahedra and FeO_5 or CoO_5 trigonal prisms. Ba (Sr) (large spheres) is located within the layers of double-octahedra and trigonal prisms. After **[14]**.

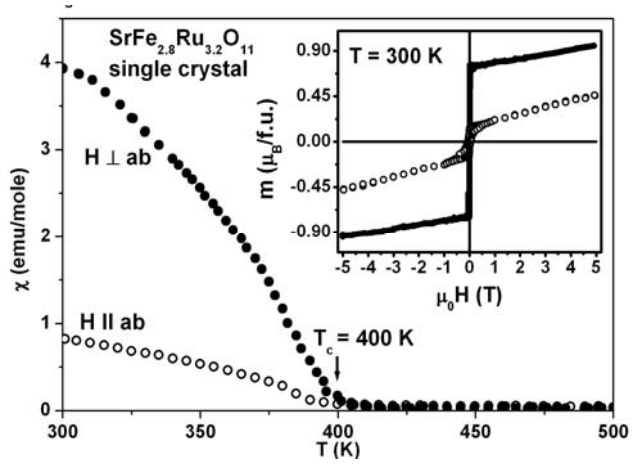

Fig. 2. Temperature dependence of the FC DC magnetic susceptibility $\chi(T)$of single-crystal $SrFe_{2.8}Ru_{3.2}O_{11}$ for **H** || **ab** and **H** ⊥ **ab** plane (easy direction) at applied magnetic field $\mu_oH = 0.1$ T. Inset shows the magnetic moment m vs. H at 300 K for the two field orientations. Arrow designates the FM ordering temperature T_c. After **[15,16]**.

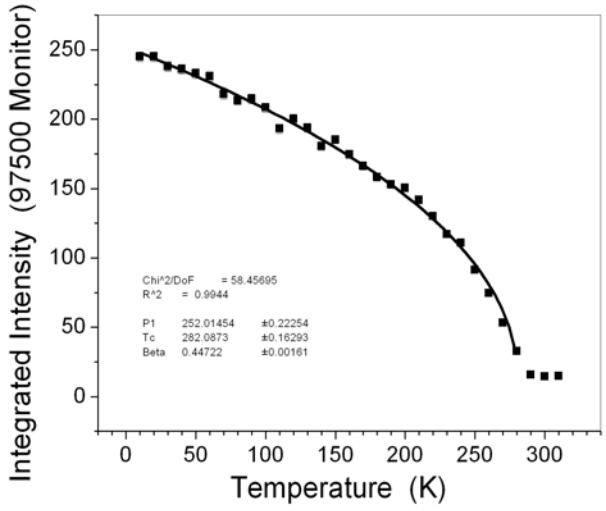

Fig. 3. Neutron counts for the (100) diffraction peak of $SrFe_{2.6}Ru_{3.4}O_{11}$ versus temperature (H = 0), which mimics the temperature dependence of our SQUID data below T_C = 300 K. The line is a power-law fit of the data, which do not follow a mean-field behavior.

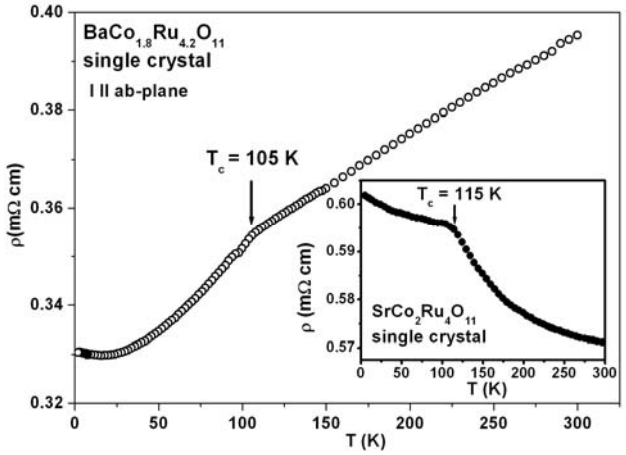

Fig. 4. ρ(T) for single-crystal $BaCo_{1.8}Ru_{4.2}O_{11}$ (**I || ab**). Inset shows ρ(T) for single-crystal $SrCo_2Ru_4O_{11}$. Arrows designate the FM magnetic ordering temperature T_c. After **[15,16]**. (Stoichiometric $BaFe_2Ru_4O_{11}$ and $BaCo_2Ru_4O_{11}$ were previously described as "poor metals", since the electrical resistivities ρ(T) of ***pressed pellets*** exhibited very weak semiconducting behavior **[18].)**

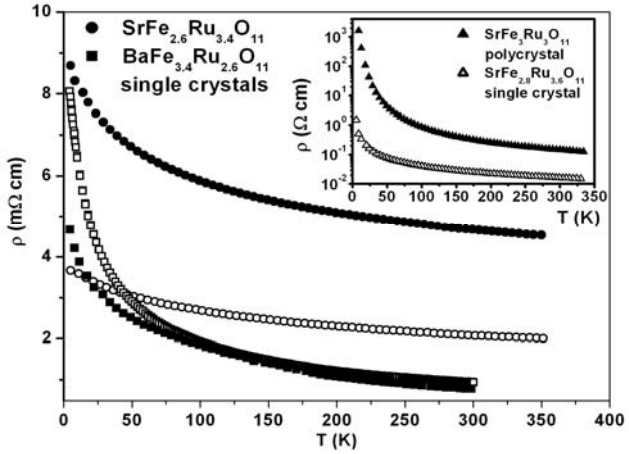

Fig. 5. Temperature dependence of resistivity ρ(T) for $BaFe_{3.4}Ru_{2.6}O_{11}$ and $SrFe_{2.6}Ru_{3.4}O_{11}$ single crystals. Filled and unfilled symbols correspond to electrical current **I** ⊥ **ab**, and **I** || **ab**, respectively. Inset shows ρ(T) for polycrystalline $SrFe_3Ru_3O_{11}$ and single-crystal $SrFe_{2.8}Ru_{3.2}O_{11}$. After **[15,16]**.

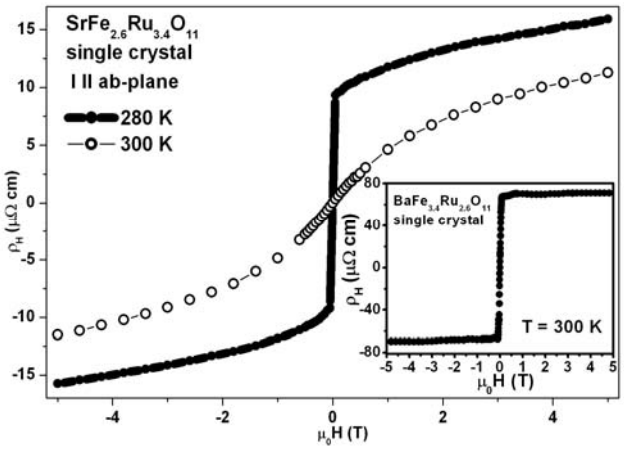

Fig. 6. Magnetic field dependence of the Hall resistivity $\rho_H(H)$ of single-crystal $SrFe_{2.6}Ru_{3.4}O_{11}$ at 280 and 300 K. The sharp change in slope at 0.1 T (anomalous Hall effect) is proof of spontaneous electron spin-polarization. Inset shows $\rho_H(H)$ for single-crystal $BaFe_{3.4}Ru_{2.6}O_{11}$ at T = 300 K. After **[15,16].**

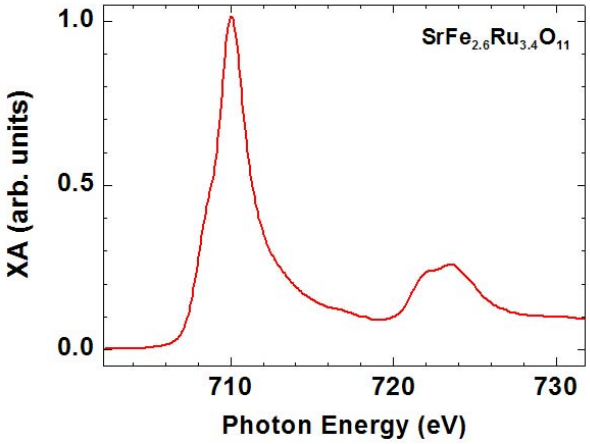

Fig. 7. Fe $L_{3,2}$ XA spectra of $SrFe_{2.6}Ru_{3.4}O_{11}$ indicating the Fe oxidation state in material is mixed 2+/3+.

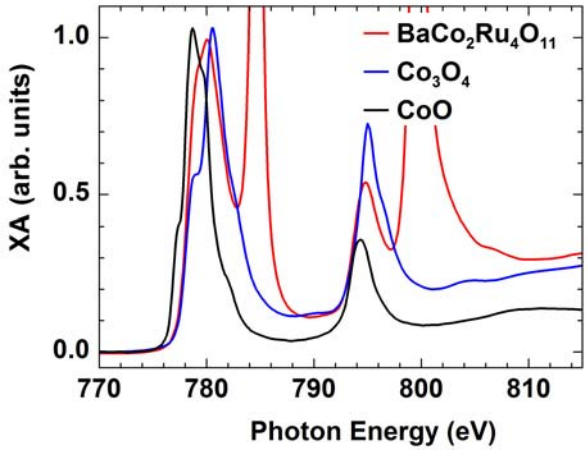

Fig. 8. Co XA spectra of $Co^{+2}(Co^{+3})_2O_4$, $Co^{+2}O$ and $BaCo_2Ru_4O_{11}$ showing the Co oxidation state in the latter material is mixed (+2/+3). The pronounced spectral features near 785eV amd 800eV in $BaCo_2Ru_4O_{11}$ are due to the Ba $M_{4,5}$ absorption edges.

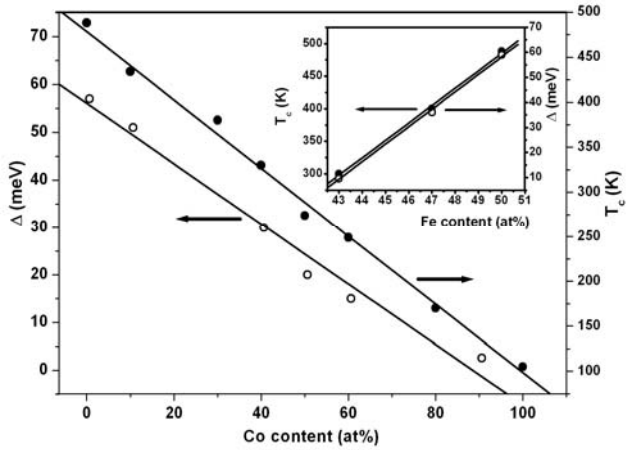

Fig. 9. Co concentration dependence of the Curie temperature T_C and semiconducting gap $\Delta$for polycrystalline $Sr(Fe_{1-y}Co_y)_{2\pm x}Ru_{4\pm x}O_{11}$ solid solutions having nominal compositions $0 \le y \le 1$, $x = 0$. **Inset:** Fe concentration dependence of T_C and $\Delta$for $SrFe_{2+x}Ru_{4-x}O_{11}$ ($x = 0.6$, 0.8 single crystals, $x = 1$ polycrystal). Solid lines are linear fits to the data. After **[15]**.

TABLE I. MAGNETIC PARAMETERS OF FE- AND CO-BEARING, R-TYPE FERRITES*

Composition	**T_C (K)**	**μ_{eff} (μ_B/f.u.)**	**$\theta_{p\perp}$ (K)**	**$\theta_{p\parallel}$ (K)**	**$H_{c\parallel}$ (Oe)**	**$H_{c\perp}$ (Oe)**	**μ_s (μ_B/f.u.)**	**$m_\perp/m_\parallel$**
$SrFe_{2.6}Ru_{3.4}O_{11}$	300				10 (280K)	10 (280K)		300 (5K)
$SrFe_{2.8}Ru_{3.2}O_{11}$	400				500 (300K)	350 (300K)		26 (5K)
$SrFe_3Ru_3O_{11}$*	488							
$SrCo_2Ru_4O_{11}$	115	2.84	106	122	30 (5K)	150 (5K)	1.9 (5K)	0.1 (5K)
$BaFe_{3.4}Ru_{2.6}O_{11}$	440				480 (300K)	92 (300K)	1.25 (300K)	1.5 (5K)
$BaCo_{1.8}Ru_{4.2}O_{11}$	105	2.78	115	70	2 (5K)	200 (5K)	1.7 (5K)	0.05 (5K)

* Parallel (||) and perpendicular ($\perp$) symbols refer to "along the **ab**-plane" (i.e., $\perp$ hexagonal **c**-axis).

** Polycrystalline sample; all other samples in **Table 1** are single crystals determined to be single phase with appropriate stoichiometries via X-ray refinements and EDX (microprobe).

TABLE II. ELECTRICAL PROPERTIES OF FE- AND CO-BEARING, R-TYPE FERRITES

Compound	**$\Delta_\parallel$ ($\Delta_\perp$) (meV)**	**ρ(300K) (Ωcm)**	**n (cm^{-3})**	**μ ($cm^2V^{-1}s^{-1}$)**	**R_s ($\mu\Omega$cm)**
$BaFe_{3.39}Ru_{2.61}O_{11}$	24(30)	$9.3x10^{-4}$	$2x10^{21}$ (300 K)	4 (300 K)	70 (300 K)
$SrFe_{2.8}Ru_{3.2}O_{11}$	36	10^{-2}			
$SrFe_3Ru_3O_{11}$*	59	10^{-1}			
$SrFe_{2.6}Ru_{3.4}O_{11}$	12(10)	$2x10^{-3}$			
$BaCo_{1.8}Ru_{4.2}O_{11}$		$4x10^{-4}$	$3x10^{20}$ (120K)	55 (150 K)	
$SrCo_2Ru_4O_{11}$	~1 ($T>T_c$)	$5.7x10^{-4}$	10^{21} (120K)	2.8 (150 K)	

* Polycrystalline material, all other samples are single crystals